

AG
T

*Algebraic & Geometric
Topology*

Volume 25 (2025)

Fully augmented links in the thickened torus

ALICE KWON



Fully augmented links in the thickened torus

ALICE KWON

We study the geometry of fully augmented link complements in the thickened torus and describe their geometric properties, generalizing the study of fully augmented links in S^3 . We classify which fully augmented links in the thickened torus are hyperbolic, and show that their complements in the thickened torus decompose into ideal right-angled torihedra. We also study volume density of fully augmented links in S^3 , defined to be the ratio of its volume and the number of augmentations. We prove the volume density conjecture for fully augmented links, which states that the volume density of a sequence of fully augmented links in S^3 which diagrammatically converges to a biperiodic link converges to the volume density of that biperiodic link. Furthermore, we show that the complement of a sequence of these links approaches the complement of the biperiodic link as a geometric limit.

57K10, 57K32, 57M50

1 Introduction

We study a class of links called *fully augmented links*. Fully augmented links in S^3 are obtained from diagrams of links in S^3 as follows. Let K be a link in S^3 with a given planar link diagram $D(K)$. We encircle each twist region (a maximal string of bigons) of $D(K)$ with a single unknotted component, called a *crossing circle*. The complement of the resulting link is homeomorphic to the link obtained by removing all *full-twists*, ie pairs of crossings from each twist region. Therefore a diagram of the fully augmented link contains a finite number of crossing circles, each encircling two strands of the link. These crossing circles are perpendicular to the projection plane and the other link components are embedded on the projection plane, except possibly for a finite number of single crossings, called *half-twists*, which are adjacent to the crossing circles; see [Figure 1](#).

The geometry of fully augmented link complements in S^3 can be explicitly described in terms of an ideal right-angled polyhedral decomposition which is closely related to the link diagram. This geometry has been studied in detail by Adams [2], Agol and D Thurston [15, Appendix], Purcell [17] and Chesebro, Deblois and Wilton [12]. In [11] Champanerkar, Kofman and Purcell studied the geometry of alternating link complements in the thickened torus and described their decompositions into torihedra, which are toroidal analogs of polyhedra. We combine the methods used to study fully augmented links in S^3 and alternating links in the thickened torus to study the geometry of fully augmented link complements in the thickened torus. We generalize many geometric properties of fully augmented links in S^3 to those in the thickened torus $T^2 \times I$, where $I = (-1, 1)$.

A *biperiodic link* \mathcal{L} is an infinite link in $\mathbb{R}^2 \times I$ with a projection on $\mathbb{R}^2 \times \{0\}$ which is invariant under an action of a two-dimensional lattice Λ by translations. The quotient $L = \mathcal{L}/\Lambda$ is a link in $T^2 \times I$ with a projection on $T^2 \times \{0\}$. This projection on $T^2 \times \{0\}$ is the link diagram of L .

Volume density of a link K was first introduced by Champanerkar, Kofman and Purcell in [10] as the ratio of its hyperbolic volume, $\text{vol}(K)$, and its crossing number, $c(K)$. In [10; 11] they studied volume densities of sequences of alternating links in S^3 which diagrammatically converge to two specific biperiodic links called the square weave and the triaxial link. They proved that volume density of such a sequence of alternating links converges to that of the corresponding biperiodic link. In general, they conjectured the following:

Conjecture 1.1 (volume density conjecture [11]) *Let \mathcal{L} be any biperiodic alternating link with alternating quotient link L . Let $\{K_n\}$ be a sequence of alternating hyperbolic links which Følner converges to \mathcal{L} . Then*

$$\lim_{n \rightarrow \infty} \frac{\text{vol}(K_n)}{c(K_n)} = \frac{\text{vol}((T^2 \times I) - L)}{c(L)}.$$

Definition 1.2 *A fully augmented biperiodic link \mathcal{L} is a fully augmented infinite link in $\mathbb{R}^2 \times I$ with a projection on $\mathbb{R}^2 \times \{0\}$ which is invariant under an action of a two-dimensional lattice Λ by translations. The quotient $L = \mathcal{L}/\Lambda$ is a fully augmented link in $T^2 \times I$ with a projection on $T^2 \times \{0\}$.*

We define the *volume density* of a fully augmented link in S^3 (with or without half-twists) to be the ratio of its volume and the number of augmentations. We similarly define volume density of fully augmented links in the thickened torus. Using the geometry of fully augmented link complements in S^3 studied previously, and our results on the geometry of fully augmented link complements in the thickened torus, we prove the volume density conjecture for fully augmented links.

In Section 2 we classify hyperbolic fully augmented links in the thickened torus.

Theorem 2.11 *Let K be a link in $T^2 \times I$ with a weakly prime, twist-reduced cellular link diagram D . Let L be a link obtained by fully augmenting D . Then $T^2 \times I - L$ decomposes into two isometric totally geodesic right-angled torihedra, and hence L is hyperbolic.*

Remark 1.3 Augmented link diagrams are link diagrams obtained by adding crossing circles to some of the twist sites of a given link diagram, and are different from fully augmented links. Kwon and Tham [14] proved that augmented links in the thickened torus are hyperbolic. A generalization to thickened surfaces was also proved by Adams, Capovilla-Searle, D Li, L Q Li, McErlean, Simons, Stewart and Wang [4]. Theorem 2.11 gives a much stronger result for fully augmented links, as it describes the right-angled geometry of the complement and uses very different proof techniques than [4; 14]. The decomposition of the link L in Theorem 2.11 into right-angled torihedra (see Definition 2.6) is very important for Theorem 3.20, which investigates limit points of volume densities of fully augmented links.

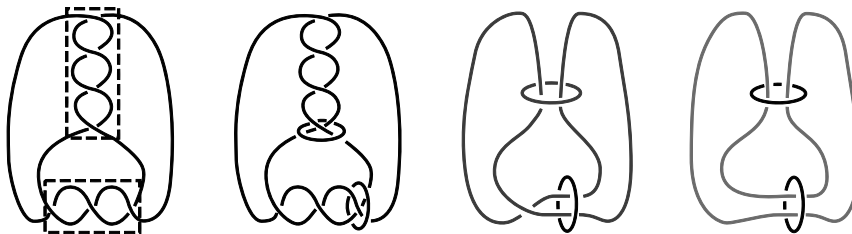


Figure 1: Left: link diagram of K . Center left: crossing circles added to each twist region. Center right: a fully augmented link diagram with all full-twists removed. Right: fully augmented link diagram with no half-twists.

In [Section 3](#) we discuss volume density and the volume density spectrum of fully augmented links in S^3 , and give many examples. In [Section 3.2](#) we define Følner convergence for fully augmented links and prove the volume density conjecture for fully augmented links. Følner convergence for links was first defined by Champanerkar, Kofman and Purcell [\[10\]](#) for alternating links; we adapt the definition of Følner convergence for sequences of fully augmented links.

Theorem 3.20 *Let \mathcal{L} be a biperiodic fully augmented link with quotient link L . Let $\{K_n\}$ be a sequence of hyperbolic fully augmented links in S^3 such that K_n Følner converges to \mathcal{L} geometrically. Then*

$$\lim_{n \rightarrow \infty} \frac{\text{vol}(K_n)}{a(K_n)} = \frac{\text{vol}((T^2 \times I) - L)}{a(L)},$$

where $a(K)$ denotes the number of augmentations of a fully augmented link K .

As an application in [Corollary 3.23](#) we show that the endpoint $10v_{\text{tet}}$ of the volume density spectrum of fully augmented links in S^3 is a limit point, by constructing a sequence of hyperbolic fully augmented links in S^3 which Følner converge everywhere to a fully augmented biperiodic link whose volume density is $10v_{\text{tet}}$.

Acknowledgments I would like to thank my advisor Abhijit Champanerkar for guidance in this paper. I would also like to thank Ilya Kofman and Jessica Purcell for helpful conversations in regards to this project.

2 Hyperbolicity of fully augmented links in the thickened torus and volume bounds

To define fully augmented links in the thickened torus we first need to define twist-reduced diagrams for links in $T^2 \times I$. Howie and Purcell defined twist-reduced diagrams for links in thickened surfaces in [\[13\]](#). However for links in the thickened torus we can also define twist-reduced diagrams using the biperiodic link diagram in \mathbb{R}^2 :

Definition 2.1 *A twist region in the biperiodic link diagram \mathcal{L} is a maximal string of bigons, or a single crossing. A twist region in the link diagram $L = \mathcal{L}/\Lambda$ is a quotient of a twist region in \mathcal{L} .*

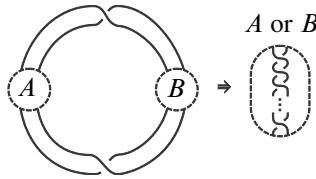


Figure 2: Twist-reduced diagram.

A biperiodic link \mathcal{L} is called *twist-reduced* if for any simple closed curve on the plane that intersects \mathcal{L} transversely in four points, with two points adjacent to one crossing and the other two points adjacent to another crossing, the simple closed curve bounds a subdiagram consisting of a (possibly empty) collection of bigons strung end-to-end between these crossings; see Figure 2. We say L is *twist-reduced* if it is the quotient of a twist-reduced biperiodic link.

Definition 2.2 A *fully augmented link diagram* in $T^2 \times I$ is a diagram of a link L that is obtained from a twist-reduced diagram K in $T^2 \times I$ as follows: augment every twist region with a circle component, called a *crossing circle*, and get rid of all full-twists; see Figure 3. A *fully augmented link* in $T^2 \times I$ is a link which has a fully augmented link diagram in $T^2 \times I$.

Remark 2.3 For fully augmented links in S^3 , depending on the parity of the number of crossings in a twist region, the fully augmented link may or may not have a half-twist at that crossing circle; see Figure 1, center right. Similarly, depending on the parity of the number of crossings at a twist region, a fully augmented link in the thickened torus may or may not have a half-twist at that crossing circle.

Definition 2.4 A graph $G = (V, E)$ on the torus is *cellular* if its complement is a collection of open disks.

Torihedra were first defined in [11] and play the role of polyhedra in polyhedral decompositions of link compliments in S^3 , eg it is proved in [11] that a complement of a link in the thickened torus decomposes into torihedra. Here we recall the definition of a torihedron.

2.1 Torihedral decomposition

Definition 2.5 A *torihedron* is a cone on the torus, $T^2 \times [0, 1]/(T^2 \times \{1\})$, with a cellular graph G on $T^2 \times \{0\}$. The edges and faces of G are called the edges and faces of the torihedron. An *ideal torihedron*

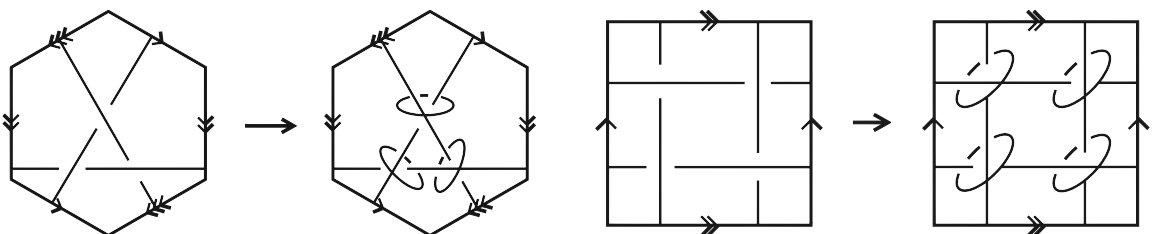


Figure 3: Left: a fully augmented triaxial link. Right: a fully augmented link on the square weave.

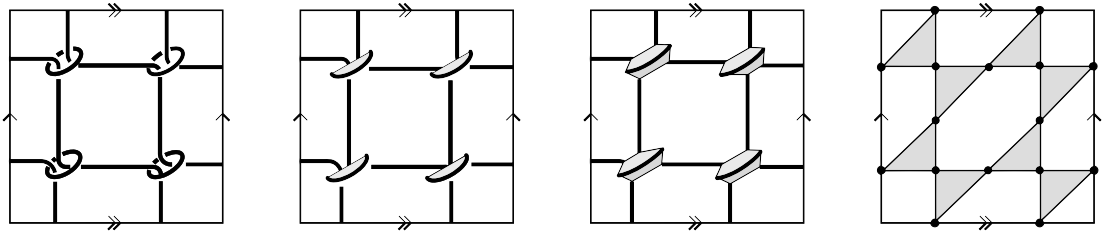


Figure 4: Left: a fundamental domain for a fully augmented square weave, L . Center left: disks cut in half at each crossing circle. Center right: sliced and flattened half-disks at each crossing circle. Right: collapsing the strands of the link and parts of the augmented circles (shown in bold) to ideal points gives the bowtie graph Γ_L . The disks become shaded bowties and the white regions become hexagons.

is a torihedron with the vertices of G and the vertex $T^2 \times \{1\}$ removed. Hence, an ideal torihedron is homeomorphic to $T^2 \times [0, 1)$ with a finite set of points (ideal vertices) removed from $T^2 \times \{0\}$. The graph G is called the *graph of the torihedron*.

Definition 2.6 An *angled torihedron* is a torihedron with an angle assignment on each edge of the graph of the torihedron. An assignment of the angle $\frac{1}{2}\pi$ on each edge is called a *right-angled torihedron*.

Proposition 2.7 Let L be a fully augmented link in $T^2 \times I$. Then there is a decomposition of the link complement $(T^2 \times I) - L$ into two combinatorially isomorphic torihedra such that

- (i) the faces of each torihedron can be checkerboard colored so that the shaded faces are triangular and arise from the bowties corresponding to crossing circles,
- (ii) the graph of each torihedron is 4-valent.

Proof We follow the cut-slice-flatten construction described in [15]. Let L be a fully augmented link in $T^2 \times I$. We begin by assuming that there are no half-twists, the crossing circles are lateral to $T^2 \times \{0\}$ and the components of L that are not crossing circles lie flat on $T^2 \times \{0\}$. There are twice-punctured disks bounded by the crossing circles which are perpendicular to the projection plane.

- (i) Cut $T^2 \times I$ along the projection surface $T^2 \times \{0\}$ into two pieces. This cuts each of the twice-punctured disks bounded by a crossing circle in half; see Figure 4, center left.
- (ii) For each of the two pieces resulting from (i), slice the middle of the halves of twice-punctured disks and flatten the half-disks out; see Figure 4, center right.
- (iii) Collapse strands of the link and parts of the augmented circles to ideal vertices in each of the two pieces; see Figure 4, right.

It follows from (i)–(iii) that each piece of the decomposition is homeomorphic to $T^2 \times [0, 1)$, with the same graph on $T^2 \times \{0\}$ with vertices deleted. Hence $(T^2 \times I) - L$ decomposes into two identical ideal torihedra.

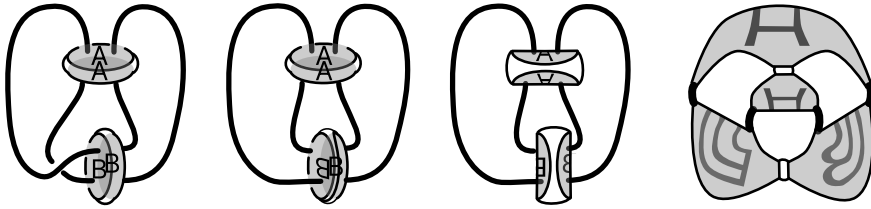


Figure 5: The gluing of the torihedra when a half-twist is present (disk B) and when a half-twist is absent (disk A). This figure, adapted from [18], is for links in S^3 , but since this is a local move the same gluing works for links in $T^2 \times I$.

After (ii), the cut-sliced-flattened half-disks become a hexagon with an edge in the middle corresponding to the strand of half of a crossing circle. Upon collapsing the crossing circle this becomes a bowtie; see Figure 4, center right and far right. Each vertex of the graph is 4-valent since it is shared by two triangles of either two different bowties or one bowtie. Again by construction, each edge is shared by a triangle of a bowtie and a polygon that does not come from a bowtie; see Figure 4, right. Hence we can shade each triangle of the bowtie to get a checkerboard coloring on the graph of the torihedron such that the shaded faces are bowties.

The two torihedra are glued together as follows: the white faces are glued to the corresponding white faces, and the bowties are glued as shown in Figure 6, left.

In the case when there is a half-twist at a crossing circle, we split the whole twice-punctured disk into two copies, and flip one of the disks to remove the half-twist. This only affects the gluing of faces of the torihedra. Hence if there are half-twists, then we get the same torihedra but with a different gluing pattern on the bowties as shown in Figure 5 and Figure 6, right. \square

Definition 2.8 For a fully augmented link L in the thickened torus, the decomposition of $T^2 \times I - L$ described above is called the *bowtie torihedral decomposition* of L . We call the graph of the torihedra the *bowtie graph* of L and denote it by Γ_L .

Lemma 2.9 Let L be a hyperbolic fully augmented link in $T^2 \times I$. The following surfaces are embedded totally geodesic surfaces in the hyperbolic structure on the link complement:

- (i) each twice-punctured disk bounded by a crossing circle,
- (ii) each connected component of the projection surface.

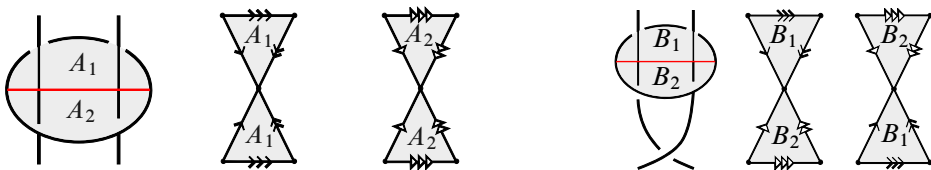


Figure 6: Left: gluing information on the edges of the bowtie without half-twists. Right: gluing information on the edges of the bowtie with half-twist.

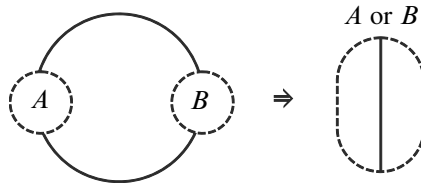


Figure 7: Prime diagram.

Proof (i) The disk E bounded by a crossing circle is punctured by two arcs of the link diagram lying on the projection plane. Adams [1] showed that any incompressible twice-punctured disk properly embedded in a hyperbolic 3-manifold is totally geodesic. Hence it suffices to show that E is incompressible. Let L be a hyperbolic fully augmented link in $T^2 \times I$. Since $T^2 \times I \simeq S^3 - H$, where H is the Hopf link, $L \cup H$ is a hyperbolic link in S^3 .

Suppose there is a compressing disk D with $\partial D \subset E$. Since ∂D is an essential closed curve on E , it must encircle one or two punctures of E . Suppose it encircles only one puncture. This means that the union of D and the disk bounded by ∂D inside the closure of E forms a sphere in S^3 met by the link exactly once. This is a contradiction to the generalized Jordan curve theorem. Hence ∂D must bound a twice-punctured disk E' on E . This means $(E - E') \cup D$ is a boundary-compressing disk for the crossing circle, contradicting the boundary irreducibility of $S^3 - (L \cup H)$.

(ii) Notice that the reflection through the projection surface $(T^2 \times \{0\})$ preserves the link complement, fixing the plane pointwise. Then it is a consequence of Mostow–Prasad rigidity that such a surface must be totally geodesic; see [17, Lemma 2.1]. \square

2.2 Hyperbolicity

Definition 2.10 Let \mathcal{L} be a bi-periodic link with diagram $D(\mathcal{L})$. We say $D(\mathcal{L})$ is prime if whenever a disk embedded in $\mathbb{R}^2 \times \{0\}$ meets $D(\mathcal{L})$ transversely in exactly two edges, then the disk contains a simple edge of the diagram and no crossings; see Figure 7.

A diagram of a link L in $T^2 \times I$, denoted by $D(L)$, is *weakly prime* if $D(L)$ is a quotient of a prime bi-periodic link diagram $D(\mathcal{L})$ in $\mathbb{R}^2 \times \{0\}$.

Theorem 2.11 Let K be a link in $T^2 \times I$ with a weakly prime twist-reduced cellular link diagram D . Let L be a link obtained by fully augmenting D . Then $T^2 \times I - L$ decomposes into two isometric totally geodesic right-angled torihedra, and hence L is hyperbolic.

The proof of Theorem 2.11 relies on a result about the existence of certain circle patterns on the torus due to Bobenko and Springborn [7]. We use similar ideas from [11] to prove Theorem 2.11

Theorem 2.12 [7] Suppose G is a 4-valent graph on the torus T^2 , and $\theta \in (0, 2\pi)^E$ is a function on edges of G that sums to 2π around each vertex. Let G^* denote the dual graph of G . Then there exists

a circle pattern on T^2 with circles circumscribing faces of G (after isotopy of G) and having exterior intersection angles θ if and only if the following condition is satisfied:

Suppose we cut the torus along a subset of edges of G^* , obtaining one or more pieces. For any piece that is a disk, the sum of θ over the edges in its boundary must be at least 2π , with equality if and only if the piece consists of only one face of G^* (only one vertex of G).

The circle pattern on the torus is uniquely determined up to similarity.

Proof of Theorem 2.11 Decompose $(T^2 \times I) - L$ into two torihedra using Proposition 2.7. Let Γ_L be the bowtie graph on $T^2 \times \{0\}$. Assign angles $\theta(e) = \frac{1}{2}\pi$ for every edge e in Γ_L . We now verify the condition of Theorem 2.12. This will prove the existence of an orthogonal circle pattern (circle pattern whose angle at the intersection of any two circles is orthogonal) circumscribing the faces of Γ_L .

Let C be a loop of edges of Γ_L^* enclosing a disk D . Suppose C intersects n edges of Γ_L transversely. Let V denote the number of vertices of Γ_L that lie in D , and let E denote the number of edges of Γ_L inside D disjoint from C . Because the vertices of Γ_L are 4-valent and since the edges inside D which are disjoint from C get counted twice for each of its end vertices, $n + 2E = 4V$. This implies n is even. Since K is weakly prime and C is made up of edges dual to Γ_L this implies $n > 2$. Since n is even, $n \geq 4$. Hence the sum of the angles for all edges of C must be at least 2π .

We now show that this is an equality if and only if C consists of one face of Γ_L^* , ie C encloses only one vertex. Suppose that $\sum_{e \in C} \theta(e) > 2\pi$. Since $\theta(e) = \frac{1}{2}\pi$ for every $e \in \Gamma_L$, and n is even, $n \geq 6$. Moreover

$$n \geq 6 \implies 4V - 2E \geq 6 \implies 2V - E \geq 3 \implies V \geq 2.$$

Hence C encloses more than one vertex.

Conversely, let $\sum_{e \in C} \theta(e) = 2\pi$. This implies $n = 4$.

Let the edges of C be e_i for $0 \leq i \leq 3$, with e_i incident to vertices v_i and v_{i+1} , and $v_0 = v_4$. Let the faces dual to v_i be F_{v_i} . Without loss of generality, let F_{v_0} be a shaded triangular face. Since Γ_L is checkerboard colored, F_{v_2} is also a shaded triangular face.

Suppose $F_{v_0} \cap F_{v_2} = \emptyset$. Then the edge e_2 must enter a white face F_{v_3} which has empty intersection with F_{v_0} ; see Figure 8, left.

Since the bowties correspond to crossing circles (see Figure 9, left) the loop C gives a loop which intersects L . At the vertex v_0 , which is in the shaded bowtie, at least one of the edges incident to v_0 has to intersect L . If only one edge at v_0 intersects L , since C bounds a disk, only one edge at v_2 intersects L , giving the case shown in Figure 9, center. Similarly if both edges incident to v_0 intersect L , since C bounds a disk, then the same is true for both edges incident at v_2 , giving the case shown in Figure 9, right. If C intersects two strands of L as in Figure 9, center, since C bounds a disk, this contradicts the weakly prime condition of K . If C intersects two strands on each side as in Figure 9, right, this will contradict the twist-reduced condition on K .

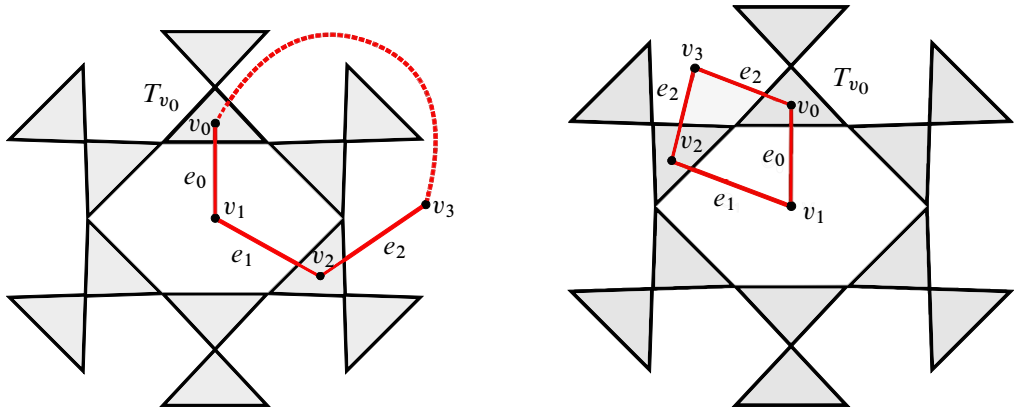


Figure 8: Left: when $n \geq 5$ and C closes with ≥ 5 edges. Right: when $n = 4$ and C closes with four edges.

Therefore $F_{v_0} \cap F_{v_2} \neq \emptyset$. Since both faces are triangles, they can only intersect in a vertex. This implies that C encloses a single vertex; see Figure 8, right.

Now, since we showed that Γ_L is a graph on the torus which satisfies the conditions of Theorem 2.12, there exists an orthogonal circle pattern on the torus with circles circumscribing the faces of Γ_L . Since a white face of the decomposition intersects any other white face only at ideal vertices, the circles which circumscribe the white faces create a circle packing, where the points of tangency are those corresponding to the associated ideal vertices. Since Γ_L is 4-valent and every edge has been assigned an angle of $\frac{1}{2}\pi$, the circles of the shaded faces meet orthogonally.

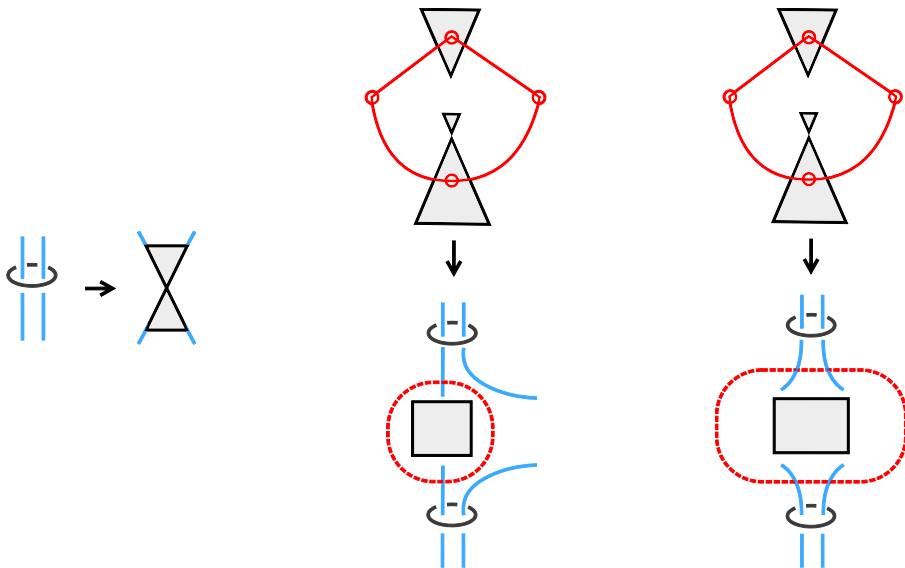


Figure 9: Left: the crossing circle splits into a bowtie. Center: C is in red. C intersects the original link in two points and hence must be a trivial edge. Right: C is in red. C can intersect the original link at four points and therefore must bound a twist region on one side.

Lifting the circle pattern to the universal cover of the torus defines an orthogonal biperiodic circle pattern on the plane. Considering the plane $z = 0$ as a part of the boundary of \mathbb{H}^3 , this circle pattern defines a right-angled biperiodic ideal hyperbolic polyhedron in \mathbb{H}^3 . The torihedron of the decomposition of $(T^2 \times I) - L$ is the quotient of \mathbb{H}^3 by $\mathbb{Z} \times \mathbb{Z}$ which is now realized as a right-angled hyperbolic torihedron. It follows from [13, Theorem 1.1] that $(T^2 \times I) - L$ is hyperbolic. \square

Remark 2.13 Adams [2] proved that fully augmented link complements in S^3 are hyperbolic. We have proved an analogous result for fully augmented link complements in $T^2 \times I$. Our method of finding an orthogonal circle pattern which circumscribed the faces of the bowtie graph can also be applied to the case of fully augmented links in S^3 . In this we have to use Andreev's theorem [19] to ensure a totally geodesic right-angled polyhedra.

2.3 Volume bounds

We show that a hyperbolic fully augmented link with c crossings in the thickened torus has an upper volume bound of $10cv_{\text{tet}}$. In the next section we show volume density convergence of fully augmented links. This means if we can find a link in the thickened torus whose volume is exactly $10cv_{\text{tet}}$ the corresponding biperiodic link will have volume density $10v_{\text{tet}}$. We will use this to show that an endpoint of the volume density spectrum of fully augmented links can be obtained as a limit.

Proposition 2.14 *Let L be a hyperbolic fully augmented link with c crossing circles. Then*

$$2cv_{\text{oct}} \leq \text{vol}(T^2 \times I - L) \leq 10cv_{\text{tet}},$$

where $v_{\text{oct}} = 3.66386\dots$ is the volume of a regular ideal octahedron and $v_{\text{tet}} = 1.01494\dots$ is the volume of a regular ideal tetrahedron.

Proof We will first prove the lower bound. By work of Adams [2], the volume of the complement of L in $T^2 \times I$ agrees with that of the fully augmented link with no half-twists. This means a lower volume bound for the complement of L in $T^2 \times I$ with half-twists will be a lower volume bound of the fully augmented link with no half-twists. Hence we will assume L has no half-twists and obtain a lower bound for $T^2 \times I - L$.

Cut $T^2 \times I - L$ along the reflection plane $T^2 \times \{0\}$, dividing it into two isometric hyperbolic manifolds. The boundary of each of these consists of the regions of L on the projection surface with punctures for the crossing circles. By Lemma 2.9 these regions are geodesic. Hence cutting along the projection surface divides $T^2 \times I - L$ into isometric hyperbolic manifolds with totally geodesic boundary.

Miyamoto showed that if N is a hyperbolic 3-manifold with totally geodesic boundary, then $\text{vol}(N) \geq -v_{\text{oct}}\chi(N)$ [16], with equality exactly when N decomposes into regular ideal octahedra. In our case, the manifold N consists of two copies of $T^2 \times [0, 1)$ with half-annuli removed for half the crossing circles.

For every half a crossing circle removed, we are removing one edge and two vertices. Hence for each crossing circle removed the Euler characteristic changes by -1 . Since there are c crossing circles, the Euler characteristic would be $-c$ for each half-cut $T^2 \times [0, 1)$. The lower bound now follows.

We now prove the upper bound. The torihedral decomposition of the link complement gives a decomposition into two identical ideal torihedra. Every triangular shaded face which comes from a bowtie corresponding to a crossing circle gives a tetrahedron when coned to the ideal vertex $T^2 \times \{1\}$ on each torihedra. Since there are c crossing circles, this gives c bowties; hence this gives $2c$ triangular shaded faces, and hence $4c$ tetrahedra. The cones on the white faces in each torihedra can be glued to make bipyramids on the white faces. These bipyramids can then be stellated into tetrahedra. Hence the number of tetrahedra coming from stellated bipyramids equals the number of edges of all the white faces. Since an edge of a white face is shared with an edge of a black triangle, this equals the number of edges of the torihedral graph, which has $6c$ edges. Hence the bipyramids on the white faces decompose into $6c$ tetrahedra. Thus the total count of tetrahedra is $4c + 6c = 10c$. Since the volume of an ideal tetrahedron is bounded by the volume of the regular ideal tetrahedron v_{tet} , the upper bound now follows. \square

Remark 2.15 In [Proposition 3.7](#) below we show that our upper bound is sharp by showing that the fully augmented square weave achieves the upper bound.

3 The volume density convergence conjecture

3.1 Volume density and its spectrum

In this section we discuss volume density of fully augmented links in S^3 , its spectrum and asymptotic behavior. Champanerkar, Kofman and Purcell [10] defined volume density of a hyperbolic link in S^3 as the ratio of the volume of the link complement to its crossing number, and studied the asymptotic behavior of the volume density for sequences of alternating links which diagrammatically converge to a biperiodic alternating link.

For a hyperbolic link L in S^3 , let $\text{vol}(L)$ denote the hyperbolic volume of $S^3 - L$. In this section we assume that all links are hyperbolic.

Definition 3.1 Let L be a fully augmented link in S^3 with or without half-twists. The *volume density* of L is defined to be the ratio of the volume of L and the number of augmentations, ie $\text{vol}(L)/a(L)$ where $a(L)$ is the number of augmentations of the link L . We similarly define the volume density of a fully augmented link in $T^2 \times I$.

Remark 3.2 Adams [2] showed that the volume of an augmented link with a half-twist at the crossing circle of the augmentation is equal to the volume without a half-twist. However, fully augmented links with and without half-twists have different crossing numbers. Hence in our definition above we divide by the number of augmentations rather than the number of crossings.

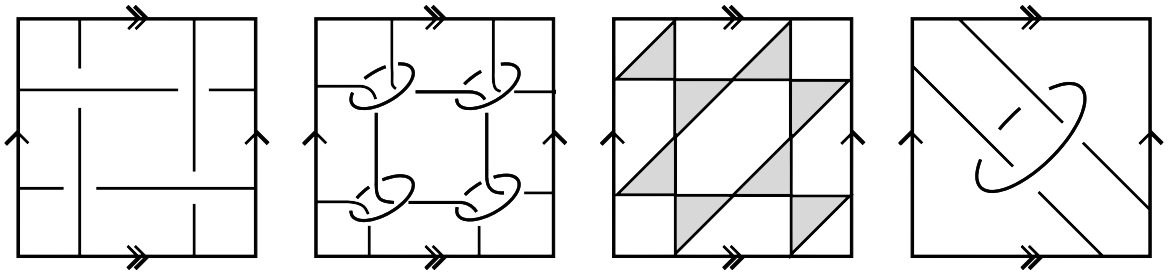


Figure 10: Left: the fundamental domain of the square weave \mathcal{W} . Center left: the fundamental domain of the fully augmented square weave, denoted by W_f . Center right: the bowtie graph Γ_{W_f} of the square weave on the left. Right: a quotient of W_f with same volume as the triaxial link.

Remark 3.3 For a fully augmented link without half-twists, the crossing number of the diagram is $4a(L)$. Thus the volume density of such a fully augmented link L is related to the volume density of L as defined in [10] by a factor of 4.

Throughout this section and the next we consider fully augmented links without half-twists.

Example 3.4 The Borromean rings B has $\text{vol}(B) = 2v_{\text{oct}}$ and $a(L) = 2$, and hence the volume density $\text{vol}(B)/a(B)$ equals v_{oct} .

Definition 3.5 The volume density spectrum of fully augmented links in S^3 is defined as $\mathcal{S}_{\text{aug}} = \{\text{vol}(L)/a(L) : L \text{ is a fully augmented link in } S^3\}$.

Proposition 3.6 The volume density spectrum \mathcal{S}_{aug} is a subset of $[v_{\text{oct}}, 10v_{\text{tet}})$.

Proof Let L be a fully augmented link. Then by [17, Proposition 3.8] the volume of L is at least $2v_{\text{oct}}(a(L) - 1)$. Since L is hyperbolic, $a(L) \geq 2$, which implies

$$\frac{\text{vol}(L)}{a(L)} \geq \frac{2v_{\text{oct}}a(L)}{a(L)} - \frac{2v_{\text{oct}}}{a(L)} > 2v_{\text{oct}}\left(1 - \frac{1}{a(L)}\right) \geq v_{\text{oct}}.$$

Since the volume density of the Borromean rings is v_{oct} , the lower bound is realized. Agol and D Thurston [15, Appendix] showed that $\text{vol}(L) \leq 10v_{\text{tet}}(a(L) - 1)$. Hence the volume density of L is at most $10v_{\text{tet}}$. \square

We show below that $10v_{\text{tet}}$ occurs as a volume density of the fully augmented square weave. Let W_f denote the fully augmented square weave as in Figure 10, center left.

Proposition 3.7
$$\frac{\text{vol}(T^2 \times I - W_f)}{a(W_f)} = 10v_{\text{tet}}.$$

Proof A fourfold quotient of W_f as shown in Figure 10, right, was studied in [8]. The authors proved that the volume of this link complement in the thickened torus is $10v_{\text{tet}}$. Hence $\text{vol}(T^2 \times I - W_f) = 40v_{\text{tet}}$, and its volume density is $10v_{\text{tet}}$. \square

Remark 3.8 The quotient of W_f as in Figure 10, right, has the same volume as that of a quotient of a triaxial link which is not a fully augmented link; see Figure 3, left. However the two links are not the same, as they have different numbers of cusps. The triaxial link has five cusps — three from each link component in the thickened torus and two from each link component of the Hopf Link — whereas the quotient of W_f in Figure 10, right, has four cusps — two from each component of the link in the thickened torus (which includes the crossing circle) and two from each link component of the Hopf Link.

3.2 Følner convergence

The volume density of the fully augmented square weave is $10v_{\text{tet}}$. We will prove below that $10v_{\text{tet}}$ is also a limit point of the \mathcal{S}_{aug} by investigating the asymptotic behavior of volume density of a sequence of fully augmented links in S^3 which diagrammatically converge to the biperiodic fully augmented square weave, as defined below. We use the notion of Følner convergence, which was first introduced in [10]. We begin by modifying its definition.

In [10] the authors used the Tait graph (checkerboard graph) of alternating links to define Følner convergence. We will use bowtie graphs to define Følner convergence for fully augmented links; see Definition 2.8 and [17, Proposition 2.2].

Definition 3.9 Let \mathcal{L} be a biperiodic fully augmented link. We will say that a sequence of fully augmented links $\{K_n\}$ in S^3 *Følner converges almost everywhere geometrically* to \mathcal{L} , denoted by $K_n \xrightarrow{\text{GF}} \mathcal{L}$, if the respective bowtie graphs $\{\Gamma_{K_n}\}$ and $\Gamma_{\mathcal{L}}$ satisfy the following: there are subgraphs $G_n \subset \Gamma_{K_n}$ such that

- (i) $G_n \subset G_{n+1}$, and $\bigcup G_n = \Gamma_{\mathcal{L}}$,
- (ii) $\lim_{n \rightarrow \infty} |\partial G_n|/|G_n| = 0$, where $|\cdot|$ denotes the number of vertices and $\partial G_n \subset \Gamma_{\mathcal{L}}$ consists of the vertices of G_n that share an edge in $\Gamma_{\mathcal{L}}$ with a vertex not in G_n ,
- (iii) $G_n \subset \Gamma_{\mathcal{L}} \cap (n\Lambda)$, where $n\Lambda$ represents n^2 copies of the fundamental domain for the lattice Λ such that $L = \mathcal{L}/\Lambda$,
- (iv) $\lim_{n \rightarrow \infty} |G_n|/3a(K_n) = 1$.

Remark 3.10 The number 3 appears in the denominator in the last condition for the definition of Følner convergence because the number of vertices of the bowtie polyhedron for K_n equals three times the number of augmentations. To see this, note that every bowtie shares two vertices with another bowtie and hence contributes three vertices to the graph. Since each bowtie corresponds to a crossing circle, the number of vertices of the graph is $3a(K)$.

Remark 3.11 Many fully augmented links can have the same bowtie graph. For example, a fully augmented link with and without half-twists have the same bowtie graph but different gluing; see Figures 11 and 12. Another example of this is when the bowtie graphs are same but with different pairing

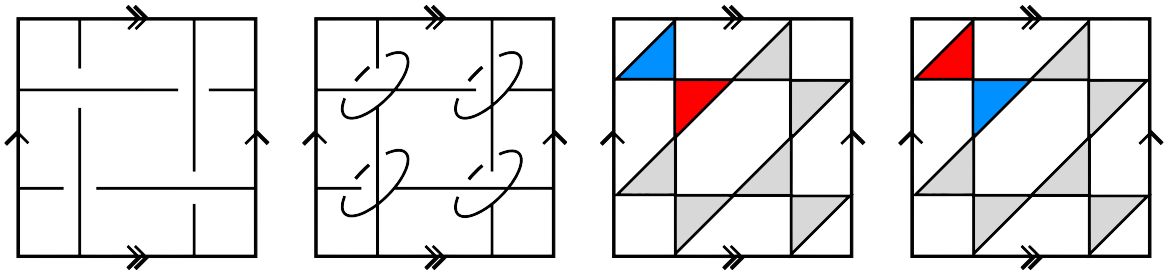


Figure 11: Left: the quotient of the square weave. Center left: W_f with half-twists at each crossing circle. Center right and far right: the bowtie graph with blue (red) face bowtie of the top torihedron being glued to a blue (red) face of the bottom torihedron

of triangles; see Figure 13 for an example of two links with same bowtie graphs but different pairings. In our definition above, we are using only the polyhedral graphs but not the pairing information of the bowties. Hence we call our Følner convergence geometric. This has the advantage of having many more sequences converging to a given biperiodic fully augmented link.

3.3 Volume density conjecture

Conjecture 3.12 (volume density conjecture) *Let \mathcal{L} be any biperiodic alternating link with alternating quotient link L . Let $\{K_n\}$ be a sequence of alternating hyperbolic links such that K_n Følner converges to \mathcal{L} . Then*

$$\lim_{n \rightarrow \infty} \frac{\text{vol}(K_n)}{c(K_n)} = \frac{\text{vol}((T^2 \times I) - L)}{c(L)}.$$

Champanerkar, Kofman and Purcell proved this conjecture when \mathcal{L} is the square weave [10] and the triaxial link [9] by finding upper and lower bounds on $\text{vol}(K_n)$ such that for a sequence of alternating links $K_n \xrightarrow{F} \mathcal{L}$, these bounds are equal in the limit. One of the key tools in their proof is the use of right-angled circle patterns. Using the right-angled decomposition of fully augmented link complements in S^3 , we construct right-angled circle patterns, and use these to prove the volume density conjecture for fully augmented links in S^3 .

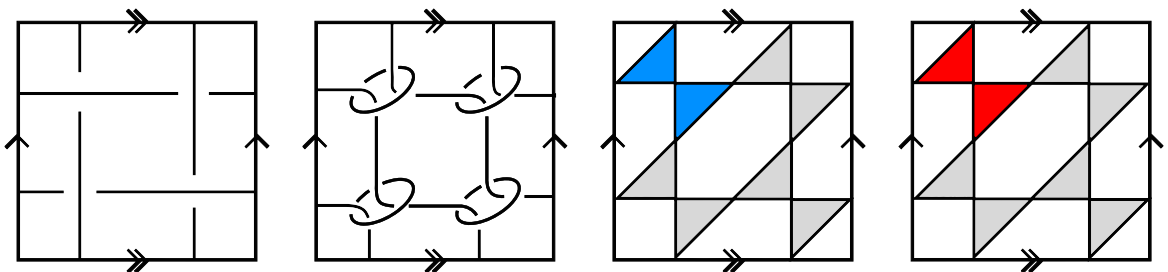


Figure 12: Left: the quotient of the square weave. Center left: W_f with no half-twists at each crossing circle. Center right and far right: the bowtie graph with blue (red) face bowtie of the top torihedron being glued to a blue (red) face of the bottom torihedron

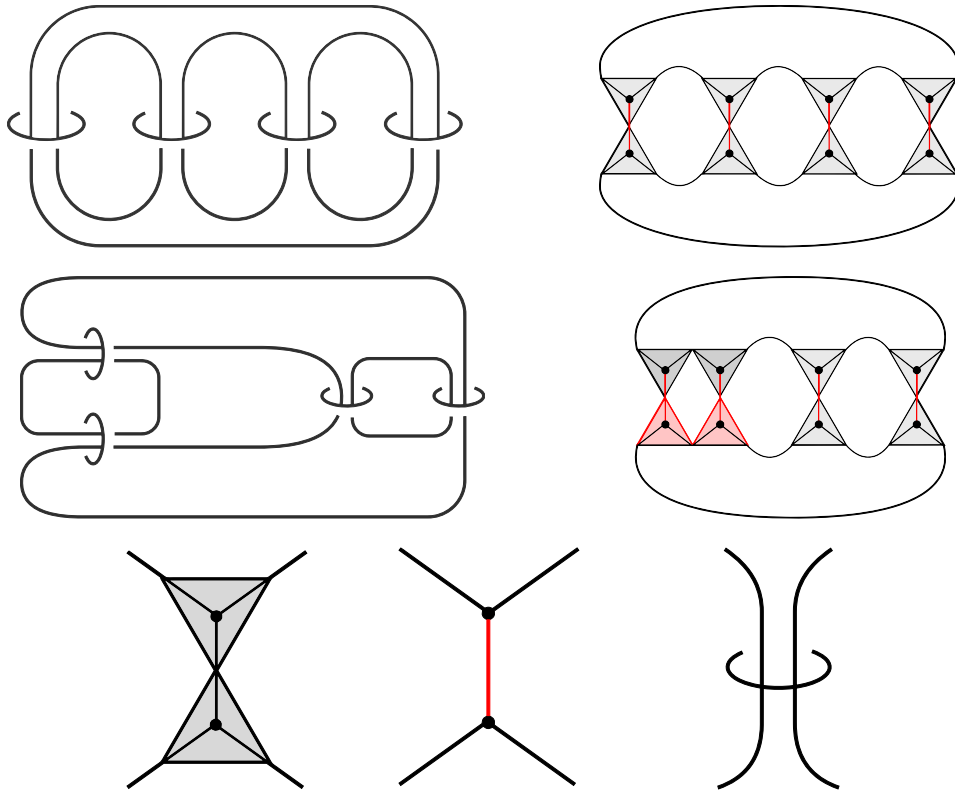


Figure 13: The fully augmented links above and below are two different links with the same bowtie graph with different pairing information.

The idea is as follows: As described in [17], each hyperbolic fully augmented link complement in S^3 can be decomposed into two right-angled ideal polyhedra which are described by a right-angled circle pattern. By Theorem 2.11 each torihedra of the bowtie torihedral decomposition is right-angled and described by another right-angled circle pattern on the torus. The $\mathbb{Z} \times \mathbb{Z}$ lift of this circle pattern is the circle pattern associated to \mathcal{L} . We show below that when a sequence of fully augmented links K_n converges to \mathcal{L} , $K_n \xrightarrow{\text{GF}} \mathcal{L}$, the circle pattern for K_n converges to an infinite circle pattern for \mathcal{L} . As a consequence we obtain the volume density convergence.

In order to work with circle patterns and convergence of circle patterns, we recall the following definitions from [5]:

Definition 3.13 A *disk pattern* is a collection of closed round disks in the plane such that no disk is the Hausdorff limit of a sequence of distinct disks and such that the boundary of any disk is not contained in the union of two other disks.

Definition 3.14 A *simply connected disk pattern* is a disk pattern in the plane such that the union of the disks is simply connected.

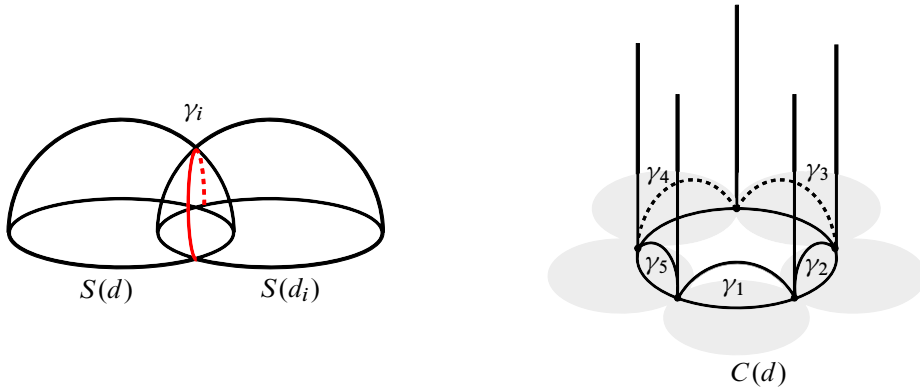


Figure 14: Left: $S(d) \cap S(d')$. Right: $C(d)$.

Let D be a disk pattern in \mathbb{C} . Let $G(D)$ be the graph with a vertex for each disk and an edge between any two vertices when the corresponding disks overlap. The graph $G(D)$ inherits an embedding in the plane from the disk pattern and we will identify $G(D)$ with its plane embedding. A face of $G(D)$ is an unbounded component of the complement of $G(D)$ in the plane. We can label the edges of $G(D)$ with the angles between the intersecting disks.

Definition 3.15 A disk pattern D is called an *ideal disk pattern* if the labels of edges of $G(D)$ are in the interval $(0, \frac{1}{2}\pi]$ and the labels around each triangle or quadrilateral in $G(D)$ sum to π or 2π , respectively.

It is clear that ideal disk patterns in \mathbb{C} correspond to ideal polyhedra in \mathbb{H}^3 , with the disks corresponding to the faces of the ideal polyhedron.

Definition 3.16 Let D and D' be disk patterns. Give $G(D)$ and $G(D')$ the path metric in which each edge has length 1. For disks d in D and d' in D' , we say (D, d) and (D', d') agree to generation n if the balls of radius n centered at vertices corresponding to d and d' admit a graph isomorphism with labels on edges preserved.

Definition 3.17 For a disk d in a disk pattern D , we let $S(d)$ be the geodesic hyperplane in \mathbb{H}^3 whose boundary agrees with that of d . That is, $S(d)$ is the Euclidean hemisphere in \mathbb{H}^3 with boundary coinciding with the boundary of d . For a disk pattern coming from a right-angled ideal polyhedron, the planes $S(d)$ form the boundary faces of the polyhedron. In this case, the disk pattern D is *simply connected* and *ideal*, since it corresponds to an ideal polyhedron.

Similarly, for a disk d in D with intersecting neighboring disks d_1, \dots, d_m , the intersection $S(d) \cap S(d_i)$ is a geodesic γ_i in \mathbb{H}^3 . The geodesics γ_i for $i = 1, \dots, m$ on $S(d)$ bound an ideal polygon in \mathbb{H}^3 . The cone of this polygon to the point at infinity is denoted by $C(d)$; see Figure 14.

Definition 3.18 A disk pattern D is said to be *rigid* if $G(D)$ has only triangular and quadrilateral faces, and each quadrilateral face has the property that the four corresponding disks of the disk pattern intersect in exactly one point.

Lemma 3.19 (Atkinson [5]) *Let D_∞ be an infinite rigid disk pattern. Then there exists a bounded sequence $0 \leq \epsilon_l \leq b < \infty$ converging to zero such that if D is a simply connected ideal rigid finite disk pattern containing a disk d such that (D_∞, d_∞) and (D, d) agree to generation l , then*

$$|\text{vol}(C(d)) - \text{vol}(C(d_\infty))| \leq \epsilon_l.$$

Note that the sequence $\{\epsilon_l\}$ in above lemma only depends on D_∞ .

Theorem 3.20 (volume density conjecture for fully augmented links) *Let \mathcal{L} be a bi-periodic fully augmented link with quotient link L . Let $\{K_n\}$ be a sequence of hyperbolic fully augmented links in S^3 . Then*

$$K_n \xrightarrow{\text{GF}} \mathcal{L} \implies \lim_{n \rightarrow \infty} \frac{\text{vol}(K_n)}{a(K_n)} = \frac{\text{vol}((T^2 \times I) - L)}{a(L)}.$$

Proof Let P_L be the bowtie torihedron with bowtie graph Γ_L of L . Let P_∞ be the infinite polyhedron in \mathbb{H}^3 which is the bi-periodic lift of P_L with its cone vertex taken to be ∞ . P_∞ can be seen to be made up of \mathbb{Z}^2 copies of an embedding of P_L in \mathbb{H}^3 with its cone vertex taken to be ∞ , glued according to the bi-periodic lift. Note that since the graph of P_L is the bowtie graph Γ_L of L , which is toroidal, the graph of P_∞ is a bi-periodic lift of Γ_L and is isomorphic to the bowtie graph $\Gamma_{\mathcal{L}}$ coming from \mathcal{L} . Let D_∞ be the infinite disk pattern coming from the infinite polyhedron P_∞ . Since P_L is a right-angled torihedron, P_∞ is also right-angled, and hence D_∞ is a right-angled disk pattern.

Since $\{K_n\}$ is a sequence of fully augmented links, each K_n is a fully augmented hyperbolic link in S^3 . The bowtie polyhedron of K_n is a right-angled ideal hyperbolic polyhedron with the same graph as the bowtie graph Γ_{K_n} . The assumption that the sequence $\{K_n\}$ Følner converges almost everywhere geometrically to \mathcal{L} implies that there are subgraphs $G_n \subset \Gamma_{K_n}$ which satisfy the conditions of Følner convergence in Definition 3.9. Hence we can embed bowtie polyhedra of K_n in \mathbb{H}^3 so that a vertex in $\Gamma_{K_n} - G_n$ is sent to infinity, and $G_n \subset G_{n+1}$. We denote this polyhedron in \mathbb{H}^3 by P_n . First note that $\text{vol}(K_n) = 2 \text{vol}(P_n)$. Let $v(P_n)$ denote the number of vertices of P_n . Since P_n is a 4-valent checkerboard graph whose shaded faces are triangles coming from the bowties, one for each augmentation, every vertex is shared by two triangles. Hence $v(P_n) = 3 \cdot 2a(K_n) \frac{1}{2} = 3a(K_n)$. Therefore,

$$\frac{\text{vol}(K_n)}{3a(K_n)} = 2 \frac{\text{vol}(P_n)}{v(P_n)}.$$

Let D_n be the disk pattern of the polyhedron P_n . It follows that D_n is a right-angled simply connected disk pattern. Since D_n corresponds to a disk pattern arising from a fully augmented link, D_n is rigid (see Definition 3.18 and Figure 15). We will now use Følner convergence to relate D_n and D_∞ .

Let F_l^n be the set of disks d in D_n such that (D_n, d) agrees to generation l but not to generation $l + 1$ with (D_∞, d_∞) . For every positive integer k , let $|f_k^n|$ denote the number of faces of P_n with k sides that are not contained in $\bigcup_l F_l^n$ and do not meet the point at infinity. By counting vertices we obtain

$$\sum_k k |f_k^n| \leq 4 |\Gamma_{K_n} - G_n|.$$

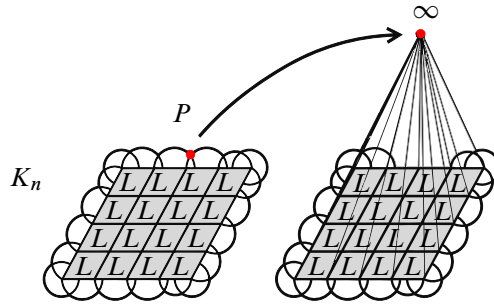


Figure 15: Left: an $n \times n$ copy of the fundamental domain of Λ with an arbitrary closure, and a marked point P on the crossing of the closure. Right: the point P moved to the cone point at ∞ .

The term $|\Gamma_{K_n} - G_n|$ counts the number of vertices that are in Γ_{K_n} but not in G_n . Since all the vertices of the graph Γ_{K_n} are 4-valent we get a factor of 4. Hence $|\Gamma_{K_n}| = v(P_n) = 3a(K_n)$, and

$$(1) \quad \lim_{n \rightarrow \infty} \frac{|G_n|}{3a(K_n)} = 1 \implies \lim_{n \rightarrow \infty} \frac{4|\Gamma_{K_n} - G_n|}{v(P_n)} = 0 \implies \lim_{n \rightarrow \infty} \frac{\sum_k k |f_k^n|}{v(P_n)} = 0.$$

Let $d \in F_l^n$ and let v_1, \dots, v_m be the vertices of G_n which lie on the boundary of d ; see Figure 16. Let $B(v, r) \subset G_n$ denote the ball centered at vertex v of radius r in the path metric on G_n . It follows from the definition of F_l^n and the fact that G_n is the planar dual of the graph of the disk pattern $G(D_n)$ — without the vertex corresponding to the unbounded face — that $d \in F_l^n$ implies $B(v_i, l) \subset G_n$ but $B(v_i, l+1) \not\subset G_n$ for $i = 1, \dots, m$. Hence the distance from v_i to ∂G_n is l , ie $v_i \in \partial B(x, l)$ for some $x \in \partial G_n$ for all $i = 1, \dots, m$.

Hence $F_l^n \subset \bigcup_{x \in \partial G_n} \partial B(x, l)$.

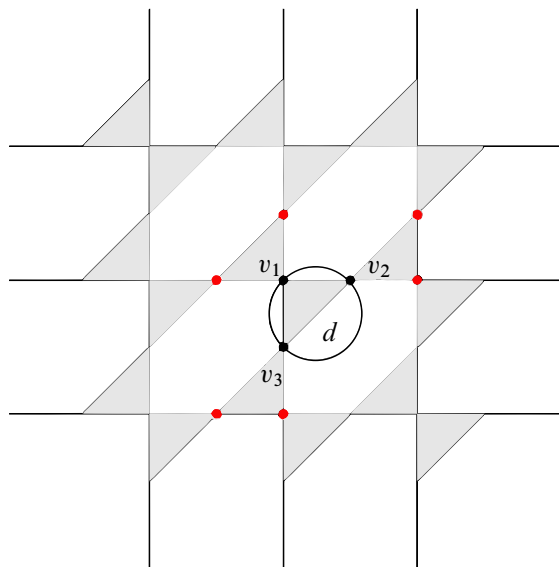


Figure 16: The circle in black is an example of $B(v_i, 1)$, and the boundary of the union over all i of $B(v_i, 1)$ is colored in red.

Lemma 3.21

$$\lim_{n \rightarrow \infty} \frac{|\bigcup_l F_l^n|}{v(P_n)} = 1.$$

Proof We begin by showing that there exists $m > 0$ such that $|\partial B(x, l)| \leq ml$ for any $x \in G_n$. By definition of Følner convergence, $G_n \subset \Gamma_{\mathcal{L}}$. Babai [6] showed that the growth rate for almost vertex-transitive graphs with one end is quadratic, that is, growth of $|B(x, l)|$ is quadratic in l . Since $\Gamma_{\mathcal{L}}$ is a biperiodic 4-valent planar graph, it satisfies the conditions of Babai's theorem, and hence has quadratic growth rate. By definition, the vertices in $\partial B(x, l)$ are incident to vertices in $B(x, l - 1)$, and hence $|\partial B(x, l)|$ has linear growth rate in l .

Thus $|F_l^n| \leq ml|\partial G_n|$ and we obtain

$$\lim_{n \rightarrow \infty} \frac{|F_l^n|}{v(P_n)} \leq \lim_{n \rightarrow \infty} \frac{ml|\partial G_n|}{3a(K_n)} = \frac{ml}{3} \lim_{n \rightarrow \infty} \frac{|\partial G_n|}{|G_n|} \frac{|G_n|}{a(K_n)} = 0.$$

Since $G_n \subset G(\mathcal{L})$, every vertex of G_n lies on a disk in F_l^n for some l , and for every disk in F_l^n there are no vertices in $G(K_n) - G_n$ which lie on the disk. Now, by assumption, $\lim_{n \rightarrow \infty} |G_n|/(3a(K_n)) = 1$. Hence $\lim_{n \rightarrow \infty} |\bigcup_l F_l^n|/v(P_n) = \lim_{n \rightarrow \infty} |G_n|/(3a(K_n)) = 1$. \square

Let f_k^n be the face with k sides that is not contained in $\bigcup_l F_l^n$ which does not meet the point at infinity. For each n , $\text{vol}(C(f_k^n)) \leq k\lambda(\frac{1}{6}\pi)$, where $\lambda(\theta)$ is the Lobachevsky function defined as

$$\lambda(\theta) = -\int_0^\theta \log |2 \sin(t)| dt,$$

whose maximum value is $\lambda(\frac{1}{6}\pi)$ [19]; see also [3].

Let E^n denote the sum of the actual volumes of all the cones over the faces f_k^n , for every integer k . Then

$$(2) \quad E^n \leq \sum_k \sum_{f_k^n} k\lambda(\frac{1}{6}\pi) = \sum_k k|f_k^n|\lambda(\frac{1}{6}\pi).$$

As mentioned before, every vertex of G_n lies on a disk in F_l^n for some l , and for every disk in F_l^n there are no vertices in $\Gamma_{K_n} - G_n$ which lie on the disk. By assumption $G_n \subset \Gamma_{\mathcal{L}} \cap (n\Lambda)$, where $n\Lambda$ represents n^2 copies of the fundamental domain for the lattice Λ such that $L = \mathcal{L}/\Lambda$.

Since the cone vertex of the torihedron for $T^2 \times I - L$ is at infinity, the disk pattern obtained from taking n^2 copies of L just extends the disk pattern from one copy of L to $n \times n$ grid, as in Figure 17. The graph for the disk pattern for n^2 copies of L intersects Γ_{K_n} in G_n , as in Figure 15.

For any face f in F_l^n , let δ_l^n be a positive number such that $\text{vol}(C(f)) = \text{vol}(C(f')) \pm \delta_l^n$, where f' is a face in the disk pattern of \mathcal{L} such that the graph isomorphism between $G(D_n)$ and $G(D_\infty)$ sends f to f' . Furthermore, we choose δ_l^n so that we can bound the sequence of δ_l^n by a sequence which will converge to zero, as in Lemma 3.19.

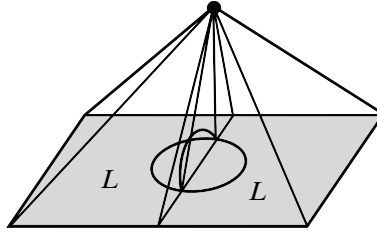


Figure 17: Two copies of the link L coned to the point at infinity. The disk pattern from one copy of L extends to the next copy.

Then

$$(3) \quad \text{vol}(P_n) = \sum_l \sum_{f \in F_l^n} (\text{vol}(f') \pm \delta_l^n) + E^n.$$

By (3) we get

$$(4) \quad \text{vol}(P_n) = \frac{1}{2}n^2 \text{vol}((T^2 \times I) - L) + \sum_l \sum_{f \in F_l^n} (\pm \delta_l^n) + E^n.$$

We divide each term by $a(K_n)$ and take the limit. For the first term of (4) we obtain

$$\lim_{n \rightarrow \infty} \frac{1}{2} \frac{n^2 \text{vol}((T^2 \times I) - L)}{a(K_n)} = \frac{1}{2} \frac{n^2 \text{vol}((T^2 \times I) - L)}{n^2 a(L)} = \frac{1}{2} \frac{\text{vol}((T^2 \times I) - L)}{a(L)}.$$

From our assumption of Følner convergence, the last condition gives us

$$\lim_{n \rightarrow \infty} \frac{a(K_n)}{n^2 a(L)} = 1.$$

By Lemma 3.19 there are positive numbers ϵ_l such that $\delta_l^n \leq \epsilon_l$, so the second term of (4) becomes

$$\lim_{n \rightarrow \infty} \frac{|\sum_l \sum_{f \in F_l^n} (\pm \delta_l^n)|}{a(K_n)} \leq \lim_{n \rightarrow \infty} \frac{\sum_l |F_l^n| \epsilon_l}{a(K_n)}.$$

Lemma 3.22

$$\lim_{n \rightarrow \infty} \frac{\sum_l |F_l^n| \epsilon_l}{a(K_n)} = 0.$$

Proof Fix any $\epsilon > 0$. Because $\lim_{l \rightarrow \infty} \epsilon_l = 0$, there is K large enough that $\epsilon_l < \frac{1}{3}\epsilon$ for $l > K$. Then $\sum_{l=1}^K \epsilon_l$ is a finite number, say M . Since we've seen above that $\lim_{n \rightarrow \infty} \bigcup_l |F_l^n|/v(P_n) = 1$ and $\lim_{n \rightarrow \infty} |F_l^n|/v(P_n) = 0$, there exists N such that if $n > N$ then $\max_{l \leq K} |F_l^n|/v(P_n) < \epsilon/(3MK)$ and $|\bigcup_l F_l^n|/v(P_n) < (1 + \epsilon)$. Then for $n > N$,

$$\frac{\sum_l |F_l^n| \epsilon_l}{v(P_n)} = \frac{\sum_{l=1}^K |F_l^n| \epsilon_l}{v(P_n)} + \frac{\sum_{l>K} |F_l^n| \epsilon_l}{v(P_n)} < \frac{\epsilon K}{3MK} + (1 + \epsilon) \frac{\epsilon}{3} < \epsilon. \quad \square$$

Now setting $v(P_n) = 3a(K_n)$ we get that the limit of the second term is zero.

Finally, by (1) and (2) we get that the third term of (4) equals zero:

$$\lim_{n \rightarrow \infty} \frac{E^n}{a(K_n)} \leq \lim_{n \rightarrow \infty} \frac{\sum_k k |f_k^n| \lambda(\frac{1}{6}\pi)}{a(K_n)} = 0.$$

Therefore $\lim_{n \rightarrow \infty} \text{vol}(P_n)/a(K_n) = \frac{1}{2} \text{vol}(T^2 \times I - L)/a(L)$, which means $\lim_{n \rightarrow \infty} \text{vol}(K_n)/a(K_n) = \text{vol}(T^2 \times I - L)/a(L)$. \square

Recall that \mathcal{W}_f denotes the fully augmented square weave link whose quotient is W_f with volume $10v_{\text{tet}}$.

Corollary 3.23 *Let K_n be any sequence of hyperbolic fully augmented links such that K_n Følner converges everywhere to \mathcal{W}_f . Then*

$$\lim_{n \rightarrow \infty} \frac{\text{vol}(K_n)}{a(K_n)} = 10v_{\text{tet}}.$$

Proof This follows from Proposition 3.7 and Theorem 3.20. \square

References

- [1] C C Adams, *Thrice-punctured spheres in hyperbolic 3-manifolds*, Trans. Amer. Math. Soc. 287 (1985) 645–656 [MR](#) [Zbl](#)
- [2] C C Adams, *Augmented alternating link complements are hyperbolic*, from “Low-dimensional topology and Kleinian groups”, Lond. Math. Soc. Lect. Note Ser. 112, Cambridge Univ. Press (1986) 115–130 [MR](#) [Zbl](#)
- [3] C Adams, A Calderon, N Mayer, *Generalized bipyramids and hyperbolic volumes of alternating k -uniform tiling links*, Topology Appl. 271 (2020) art. id. 107045 [MR](#) [Zbl](#)
- [4] C Adams, M Capovilla-Searle, D Li, L Q Li, J McErlean, A Simons, N Stewart, X Wang, *Augmented cellular alternating links in thickened surfaces are hyperbolic*, Eur. J. Math. 9 (2023) art. id. 100 [MR](#) [Zbl](#)
- [5] C K Atkinson, *Volume estimates for equiangular hyperbolic Coxeter polyhedra*, Algebr. Geom. Topol. 9 (2009) 1225–1254 [MR](#) [Zbl](#)
- [6] L Babai, *The growth rate of vertex-transitive planar graphs*, from “Proceedings of the eighth annual ACM–SIAM symposium on discrete algorithms”, ACM, New York (1997) 564–573 [MR](#) [Zbl](#)
- [7] A I Bobenko, B A Springborn, *Variational principles for circle patterns and Koebe’s theorem*, Trans. Amer. Math. Soc. 356 (2004) 659–689 [MR](#) [Zbl](#)
- [8] A Champanerkar, D Futer, I Kofman, W Neumann, J S Purcell, *Volume bounds for generalized twisted torus links*, Math. Res. Lett. 18 (2011) 1097–1120 [MR](#) [Zbl](#)
- [9] A Champanerkar, I Kofman, *Determinant density and biperiodic alternating links*, New York J. Math. 22 (2016) 891–906 [MR](#) [Zbl](#)
- [10] A Champanerkar, I Kofman, J S Purcell, *Geometrically and diagrammatically maximal knots*, J. Lond. Math. Soc. 94 (2016) 883–908 [MR](#) [Zbl](#)

- [11] **A Champanerkar, I Kofman, JS Purcell**, *Geometry of biperiodic alternating links*, J. Lond. Math. Soc. 99 (2019) 807–830 [MR](#) [Zbl](#)
- [12] **E Chesebro, J DeBlois, H Wilton**, *Some virtually special hyperbolic 3-manifold groups*, Comment. Math. Helv. 87 (2012) 727–787 [MR](#) [Zbl](#)
- [13] **JA Howie, JS Purcell**, *Geometry of alternating links on surfaces*, Trans. Amer. Math. Soc. 373 (2020) 2349–2397 [MR](#) [Zbl](#)
- [14] **A Kwon, YH Tham**, *Hyperbolicity of augmented links in the thickened torus*, J. Knot Theory Ramifications 31 (2022) art. id. 2250025 [MR](#) [Zbl](#)
- [15] **M Lackenby**, *The volume of hyperbolic alternating link complements*, Proc. Lond. Math. Soc. 88 (2004) 204–224 [MR](#) [Zbl](#) With an appendix by I Agol and D Thurston
- [16] **Y Miyamoto**, *Volumes of hyperbolic manifolds with geodesic boundary*, Topology 33 (1994) 613–629 [MR](#) [Zbl](#)
- [17] **JS Purcell**, *An introduction to fully augmented links*, from “Interactions between hyperbolic geometry, quantum topology and number theory”, Contemp. Math. 541, Amer. Math. Soc., Providence, RI (2011) 205–220 [MR](#) [Zbl](#)
- [18] **JS Purcell**, *Hyperbolic knot theory*, Graduate Studies in Math. 209, Amer. Math. Soc., Providence, RI (2020) [MR](#) [Zbl](#)
- [19] **WP Thurston**, *The geometry and topology of three-manifolds*, lecture notes, Princeton University (1979) Available at <https://url.msp.org/gt3m>

Science Department, SUNY Maritime
Throggs Neck, NY, United States

akwon@sunymaritime.edu

Received: 19 August 2022 Revised: 22 May 2023

ALGEBRAIC & GEOMETRIC TOPOLOGY

msp.org/agt

EDITORS

PRINCIPAL ACADEMIC EDITORS

John Etnyre
etnyre@math.gatech.edu
Georgia Institute of Technology

Kathryn Hess
kathryn.hess@epfl.ch
École Polytechnique Fédérale de Lausanne

BOARD OF EDITORS

Julie Bergner	University of Virginia jeb2md@eservices.virginia.edu	Thomas Koberda	University of Virginia thomas.koberda@virginia.edu
Steven Boyer	Université du Québec à Montréal cohf@math.rochester.edu	Markus Land	LMU München markus.land@math.lmu.de
Tara E Brendle	University of Glasgow tara.brendle@glasgow.ac.uk	Christine Lescop	Université Joseph Fourier lescop@ujf-grenoble.fr
Indira Chatterji	CNRS & Univ. Côte d'Azur (Nice) indira.chatterji@math.cnrs.fr	Norihiko Minami	Yamato University minami.norihiko@yamato-u.ac.jp
Octav Cornea	Université de Montreal cornea@dms.umontreal.ca	Andrés Navas	Universidad de Santiago de Chile andres.navas@usach.cl
Alexander Dranishnikov	University of Florida dranish@math.ufl.edu	Robert Oliver	Université Paris 13 bobol@math.univ-paris13.fr
Tobias Ekholm	Uppsala University, Sweden tobias.ekholm@math.uu.se	Jessica S Purcell	Monash University jessica.purcell@monash.edu
Mario Eudave-Muñoz	Univ. Nacional Autónoma de México mario@matem.unam.mx	Birgit Richter	Universität Hamburg birgit.richter@uni-hamburg.de
David Futер	Temple University dfuter@temple.edu	Jérôme Scherer	École Polytech. Féd. de Lausanne jerome.scherer@epfl.ch
John Greenlees	University of Warwick john.greenlees@warwick.ac.uk	Vesna Stojanoska	Univ. of Illinois at Urbana-Champaign vesna@illinois.edu
Ian Hambleton	McMaster University ian@math.mcmaster.ca	Zoltán Szabó	Princeton University szabo@math.princeton.edu
Matthew Hedden	Michigan State University mhedden@math.msu.edu	Maggy Tomova	University of Iowa maggy-tomova@uiowa.edu
Kristen Hendricks	Rutgers University kristen.hendricks@rutgers.edu	Daniel T Wise	McGill University, Canada daniel.wise@mcgill.ca
Hans-Werner Henn	Université Louis Pasteur henn@math.u-strasbg.fr	Lior Yanovski	Hebrew University of Jerusalem lior.yanovski@gmail.com
Daniel Isaksen	Wayne State University isaksen@math.wayne.edu		

See inside back cover or msp.org/agt for submission instructions.

The subscription price for 2025 is US \$760/year for the electronic version, and \$1110/year (+\$75, if shipping outside the US) for print and electronic. Subscriptions, requests for back issues and changes of subscriber address should be sent to MSP. Algebraic & Geometric Topology is indexed by [Mathematical Reviews](#), [Zentralblatt MATH](#), [Current Mathematical Publications](#) and the [Science Citation Index](#).

Algebraic & Geometric Topology (ISSN 1472-2747 printed, 1472-2739 electronic) is published 9 times per year and continuously online, by Mathematical Sciences Publishers, c/o Department of Mathematics, University of California, 798 Evans Hall #3840, Berkeley, CA 94720-3840. Periodical rate postage paid at Oakland, CA 94615-9651, and additional mailing offices. POSTMASTER: send address changes to Mathematical Sciences Publishers, c/o Department of Mathematics, University of California, 798 Evans Hall #3840, Berkeley, CA 94720-3840.

AGT peer review and production are managed by EditFlow[®] from MSP.

PUBLISHED BY

 **mathematical sciences publishers**

nonprofit scientific publishing

<https://msp.org/>

© 2025 Mathematical Sciences Publishers

ALGEBRAIC & GEOMETRIC TOPOLOGY

Volume 25 Issue 3 (pages 1265–1915) 2025

A-polynomials, Ptolemy equations and Dehn filling	1265
JOSHUA A HOWIE, DANIEL V MATHEWS and JESSICA S PURCELL	
The Alexandrov theorem for $2 + 1$ flat radiant spacetimes	1321
LÉO MAXIME BRUNSWIC	
Real algebraic overtwisted contact structures on 3-spheres	1377
ŞEYMA KARADERELI and FERİT ÖZTÜRK	
Fully augmented links in the thickened torus	1411
ALICE KWON	
Unbounded \mathfrak{sl}_3 -laminations and their shear coordinates	1433
TSUKASA ISHIBASHI and SHUNSUKE KANO	
Bridge trisections and Seifert solids	1501
JASON JOSEPH, JEFFREY MEIER, MAGGIE MILLER and ALEXANDER ZUPAN	
Random Artin groups	1523
ANTOINE GOLDSBOROUGH and NICOLAS VASKOU	
A deformation of Asaeda–Przytycki–Sikora homology	1545
ZHENKUN LI, YI XIE and BOYU ZHANG	
Cubulating a free-product-by-cyclic group	1561
FRANÇOIS DAHMANI and SURAJ KRISHNA MEDA SATISH	
Virtual domination of 3-manifolds, III	1599
HONGBIN SUN	
The Kakimizu complex for genus one hyperbolic knots in the 3-sphere	1667
LUIS G VALDEZ-SÁNCHEZ	
Band diagrams of immersed surfaces in 4-manifolds	1731
MARK HUGHES, SEUNGWON KIM and MAGGIE MILLER	
Anosov flows and Liouville pairs in dimension three	1793
THOMAS MASSONI	
Hamiltonian classification of toric fibres and symmetric probes	1839
JOÉ BRENDEL	
An example of higher-dimensional Heegaard Floer homology	1877
YIN TIAN and TIANYU YUAN	
Fibered 3-manifolds and Veech groups	1897
CHRISTOPHER J LEININGER, KASRA RAFI, NICHOLAS ROUSE, EMILY SHINKLE and YVON VERBERNE	